Pseudomonas cepacia 3-Hydroxybenzoate 6-Hydroxylase: Stereochemistry, Isotope Effects, and Kinetic Mechanism†

Yimin Yu, Lee-Ho Wang,‡ and Shiao-Chun Tu*
Department of Biochemical and Biophysical Sciences, University of Houston—University Park, Houston, Texas 77004
Received August 1, 1986; Revised Manuscript Received October 21, 1986

ABSTRACT: A neutral flavin semiquinone species was formed upon photoreduction of *Pseudomonas cepacia* 3-hydroxybenzoate 6-hydroxylase whereas no flavin radical was detected by anaerobic reduction with NADH in the presence of *m*-hydroxybenzoate. In the latter case, the formation of flavin semiquinone is apparently thermodynamically unfavorable. A stereospecificity for the abstraction of the 4*R*-position hydrogen of NADH has been demonstrated for this hydroxylase. Deuterium and tritium isotope effects were observed with (4*R*)-[4-^{2}H]NADH and (4*R*)-[4-^{3}H]NADH as substrates. The ^DV effect indicates the existence of at least one slow step after the isotope-sensitive enzyme reduction by dihydropyridine nucleotide. A minimal kinetic mechanism has been deduced on the basis of initial velocity measurements and studies on deuterium and tritium isotope effects. Following this scheme, *m*-hydroxybenzoate and NADH bind to the hydroxylase in a random sequence. The flavohydroxylase is reduced by NADH, and NAD^+ is released. Oxygen subsequently binds to and reacts with the reduced flavohydroxylase–*m*-hydroxybenzoate complex. Following the formation and release of water and gentisate, the oxidized holoenzyme is regenerated. The enzyme has a small (~2-fold) preference for the release of NADH over *m*-hydroxybenzoate from the enzyme–substrates ternary complex.

Flavoprotein external monooxygenases utilize NAD(P)H, or $FMNH_2$ in the case of bacterial luciferase, as an external reductant in catalyzing the activation of molecular oxygen. Subsequently, one oxygen atom is inserted into a substrate and the second atom of molecular oxygen is reduced to water. Through enzyme mechanistic investigations [Massey and Hemmerich (1975), Ballou (1984), and Hastings (1978) and references cited therein] and chemical model studies (Kemal & Bruice, 1976; Kemal et al., 1977; Ball & Bruice, 1980; Bruice, 1984), a substantial body of knowledge has already been accumulated concerning the nature of molecular oxygen activation by flavohydroxylase for substrate oxygenation. However, flavohydroxylases exhibit considerably diverse kinetic mechanisms (Wang & Tu, 1984), and much remains to be explored concerning the chemical mechanisms of hydroxylase reactions.

In the preceding paper (Wang et al., 1987), we report the induction of 3-hydroxybenzoate 6-hydroxylase (referred to as *m*-hydroxybenzoate hydroxylase hereon) in *Pseudomonas cepacia* cells and describe the isolation and general characterization of this enzyme. This hydroxylase is unique in that a new hydroxyl group is inserted into the aromatic substrate at a position para to the existing hydroxyl function whereas all other aromatic flavohydroxylases insert the new hydroxyl group at a position immediately adjacent to an existing one. Prior to our work, the isolation of a different species of 3-hydroxybenzoate 6-hydroxylase has been described (Groseclose & Ribbons, 1973), but no mechanistic study has ever been carried out. In this study, we have examined several aspects of spectral and mechanistic properties of the *P. cepacia m*-hydroxybenzoate hydroxylase. The hydroxylase was investigated with respect to anaerobic reductions, and the formation of neutral flavin semiquinone was observed under certain conditions. The stereospecificity for NADH oxidation has been established. Large deuterium and tritium isotope effects were observed for (4*R*)-[4-^{2}H]- and (4*R*)-[4-^{3}H]NADH, indicating the importance of pyridine nucleotide oxidation in the regulation of overall catalytic reaction velocity. On the basis of isotope effects and steady-state measurements, a minimal kinetic mechanism has been identified for this hydroxylase.

Experimental Procedures

Materials. *m*-Hydroxybenzoic acid was obtained from Aldrich and was recrystallized twice from hot water. NADH, dithiothreitol, FAD, and horse liver alcohol dehydrogenase were all purchased from Sigma. FAD was further purified by DEAE-cellulose chromatography (Massey & Swoboda, 1963). DEAE-cellulose DE-52 was obtained from Whatman. Hen egg white lysozyme and porcine heart diaphorase were from Boehringer-Mannheim GmbH. Concentrations of the following compounds were determined spectrophotometrically with extinction coefficients, in M^{-1} cm^{-1}, of 6220 at 340 nm for NADH, 2290 at 288 nm for *m*-hydroxybenzoate, and 11 300 at 450 nm for FAD. *m*-Hydroxybenzoate hydroxylase was purified as described in the preceeding paper. Protein concentrations were determined by the method of Lowry (1951) with lysozyme as a standard.

Preparation of Isotopically Labeled NADH. (4*R*)-[4-^{2}H]NADH was prepared by the equine liver alcohol dehydrogenase catalyzed reduction of NAD^+ with [U-^{2}H]ethanol (99% from Merck Sharp & Dohme) as a substrate. The method of Oppenheimer et al. (1971) was followed except that the final purification of (4*R*)-[4-^{2}H]NADH was achieved by chromatography on a DEAE-cellulose column preequilibrated with water and eluted with a gradient of water to 0.23 M KP_i, pH 8.2. NADH was similarly purified. By use of the same alcohol dehydrogenase, (4*S*)-[4-^{3}H]NADH was obtained by reduction of [4-^{3}H]NAD^+ (from Amersham) with ethanol as a substrate. The method of Oppenheimer et al. (1971) was modified to prepare (4*R*)-[4-^{3}H]NADH by the diaphorase-catalyzed reduction of [4-^{3}H]NAD^+ in H_2O medium. The

† This work was supported by Grants GM25953 from the National Institute of General Medical Sciences and E-1030 from The Robert A. Welch Foundation. S.-C.T. also acknowledges the support of Research Career Development Award KO4 ES00088 from the National Institute of Environmental Health Sciences.
‡ Present address: Department of Cell Biology, Baylor College of Medicine, Houston, TX 77030.

0006-2960/87/0426-1105$01.50/0

final (4*R*)-[4-^{3}H]NADH and (4*S*)-[4-^{3}H]NADH products had specific radioactivities of 1.32 and 1.02 mCi/mmol, respectively.

Anaerobic Reductions. Anaerobic spectral experiments were carried out at 23 °C with an apparatus described previously (Williams et al., 1979). Anaerobiosis was achieved by at least eight cycles of alternate evacuation and reequilibration with nitrogen freed from oxygen by passage over a BASF (Ace Glass Co.) column at 150 °C. Photoreduction of *m*-hydroxybenzoate hydroxylase was carried out by irradiation of the enzyme in 20 mM KP_i containing 2.5 mM dithiothreitol and 10 mM EDTA[1] with a (22-W, 19-cm diameter circular) fluorescent lamp placed about 8 cm from the sample cuvette. Alternatively, anaerobic enzyme solutions were titrated with a NADH stock solution from a side arm of the apparatus. Spectra were recorded with a Perkin-Elmer 552 absorption spectrophotometer interfaced to a Northstar Horizon microcomputer.

Steady-State Kinetic Analysis. Enzyme activities were determined at 23 °C in 20 mM KP_i, pH 7.6, spectrophotometrically at 340 nm. Alternatively, enzyme activities in the presence of high concentrations of NADH or (4*R*)-[4-^{2}H]-NADH were determined by monitoring oxygen consumptions on a Gilson oxygraph model 5/6. Definitions of activity units are described in the preceeding paper. The determination of apparent K_m, V_{max}, and V/K were based on statistical analysis of initial rate data with the HYPER program described by Cleland (1979) translated to BASIC for use on a Northstar Horizon computer (Ahn & Klinman, 1983).

Kinetic Isotope Effects. V_{max} and V/K were determined as described above with either NADH or (4*R*)-[4-^{2}H]NADH as a substrate, and values of ^DV and $^D(V/K)$ effects were subsequently calculated. $^D(V/K_{NH})$ was determined, by the spectrophotometric assay, at saturating *m*-hydroxybenzoate and variable (labeled or nonlabeled) NADH concentration. Alternatively, $^D(V/K_{MHB})$ was determined, by the oxygen consumption assay, at saturating (labeled or nonlabeled) NADH and variable *m*-hydroxybenzoate concentration. ^DV effects were determined by both of the assay methods described above. $^T(V/K_{NH})$ effects, referred to as $^T(V/K)$ hereon, were determined at several levels of *m*-hydroxybenzoate with (4*R*)-[4-^{3}H]NADH as a cosubstrate. The progress of the reaction was monitored by following absorbance changes at 340 nm, and the fractional conversions of substrate to product (f) were calculated. At different times, 50-μL aliquots were withdrawn, and each was applied to a DEAE-cellulose column (preswollen Whatman DE-52, 0.5 × 3.5 cm, equilibrated with water) and washed with 1.5 mL of H_2O to elute all tritiated water. The specific radioactivity of the product formed at a designated time point (R) was calculated from the amount of tritium released into water (in μCi) and the micromoles of NADH oxidized. In all cases, data were collected for $f < 0.2$, and $^T(V/K)$ effects were calculated (Northrop, 1975) according to

$$^T(V/K) = \frac{\log (1 - f)}{\log (1 - fR/R_0)} \quad (1)$$

where R_0 is the specific radioactivity of the initial (4*R*)-[4-^{3}H]NADH substrate.

RESULTS

Anaerobic Reduction. Figure 1 shows the spectral changes of *m*-hydroxybenzoate hydroxylase upon anaerobic titration by NADH. The oxidized hydroxylase was progressively reduced at increasing levels of NADH, with the full reduction of bound FAD occurring at a point corresponding to an equal molar quantity addition of NADH. The presence of one FAD per hydroxylase molecule was thus demonstrated. The absence of any absorption above 530 nm and the well-defined isosbestic point at 337 nm during the reduction by NADH indicated that no flavin semiquinone or charge-transfer complex species was detectable under our experimental conditions.

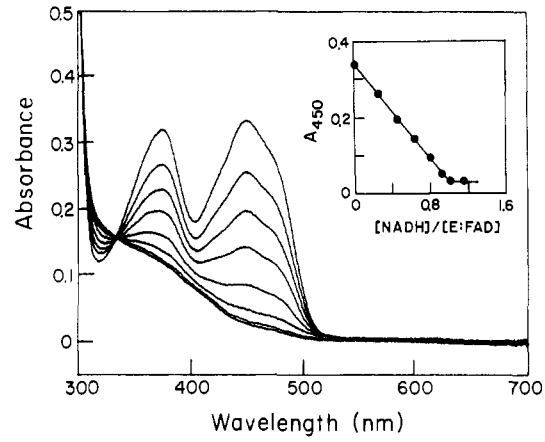

FIGURE 1: Anaerobic reduction of *m*-hydroxybenzoate hydroxylase by NADH. *m*-Hydroxybenzoate hydroxylase (29.6 nmol) in 1.0 mL of 20 mM KP_i, pH 7.6, containing 0.5 mM *m*-hydroxybenzoate was titrated anaerobically with aliquots from an anaerobic NADH (0.97 mM) stock solution. Each spectrum was recorded after equilibrium was reached. The spectra with the highest and lowest absorption at 450 nm correspond to that for the fully oxidized and two-electron reduced enzyme, respectively. (Inset) The reduction of enzyme, indicated as the decrease of absorption at 450 nm, is plotted as a function of the molar ratio of NADH added over the total enzyme-bound flavin.

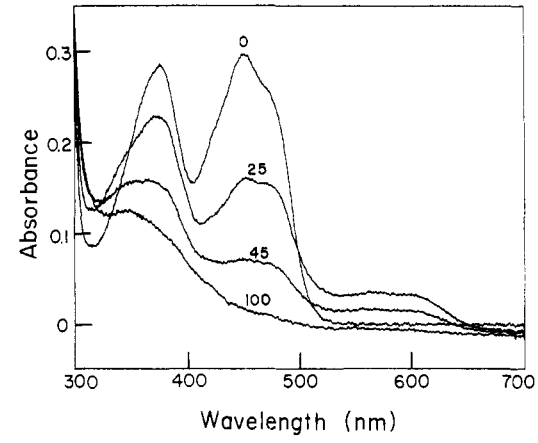

FIGURE 2: Photoreduction of *m*-hydroxybenzoate hydroxylase. The reaction solution contained 26 μM hydroxylase, 10 mM EDTA, 0.5 mM dithiothreitol, and 20 mM KP_i, pH 6.75. After anaerobiosis was achieved, the enzyme was subject to photoreduction, and spectra were recorded at different times. The time of illumination is indicated (in min) above each spectrum.

Anaerobic reduction of *m*-hydroxybenzoate hydroxylase was also carried out photochemically at pH 6.75 in the presence of EDTA (Figure 2). Contrary to the NADH reduction, the initial photoreduction of hydroxylase was accompanied by an increase in absorption above 500 nm characteristic of a neutral semiquinone (Massey & Palmer, 1966). Further irradiation resulted in the full reduction of the enzyme and the disappearance of the long-wavelength absorption. The original oxidized flavin spectrum was immediately recovered upon admission of air. Such spectral changes were also observed in the prescence of 0.5 mM *m*-hydroxybenzoate. Interestingly,

[1] Abbreviations: NH, NADH; MHB, *m*-hydroxybenzoate; OX, oxygen; EDTA, ethylenediaminetetraacetic acid.

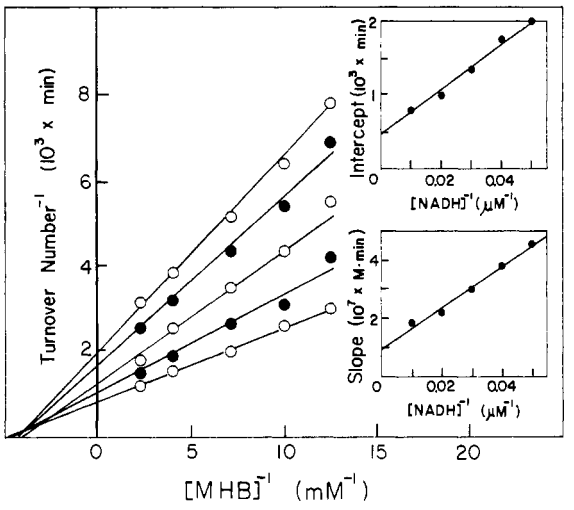

FIGURE 3: Lineweaver–Burk plots of initial velocity vs. *m*-hydroxybenzoate concentration at a constant level of oxygen and several fixed amounts of NADH. Reactions were carried out in 1 mL of 20 mM KP_i, pH 7.6, containing 2 μg of *m*-hydroxybenzoate hydroxylase, 0.24 mM O_2, and varying amounts of *m*-hydroxybenzoate as indicated. Each titration experiment was carried out at a fixed level of NADH. The concentrations of NADH were 20, 25, 33, 50, and 100 μM for lines from top to bottom. Secondary plots of ordinate intercept vs. reciprocal NADH concentration and slope vs. reciprocal NADH concentration are shown in the insets.

we have also noted that photochemical conversion of the neutral semiquinone to the fully reduced enzyme was markedly retarded at pH 7.6. Over the course of 1 h of irradiation, no significant conversion of semiquinone to fully reduced enzyme was observed.

Steady-State Kinetics. Analyses of steady-state initial velocities were carried out to determine the kinetic mechanism of *m*-hydroxybenzoate hydroxylase. When concentrations of *m*-hydroxybenzoate were varied at a constant level of oxygen and several fixed amounts of NADH, double-reciprocal plots of initial velocities vs. *m*-hydroxybenzoate concentration show a family of converging lines (Figure 3). The same pattern of double-reciprocal plots was also obtained when initial rates were analyzed as a function of NADH concentration at a constant level of oxygen and several fixed amounts of *m*-hydroxybenzoate. These results unambiguously indicate that *m*-hydroxybenzoate and NADH can bind to the same enzyme species to form a ternary complex.

In similar experiments, initial rates were analyzed as a function of *m*-hydroxybenzoate concentration at a constant amount of NADH and several fixed levels of oxygen (Figure 4) and as a function of NADH concentration at a constant level of *m*-hydroxybenzoate and several fixed amounts of O_2 (Figure 5). In both cases, parallel lines were obtained from double-reciprocal plots. Such graphic patterns indicate a ping-pong mechanism; i.e., oxygen does not bind to the same enzyme form that binds *m*-hydroxybenzoate and/or NADH.

We interpret these kinetic results by proposing that the oxidized enzyme forms a ternary complex with *m*-hydroxybenzoate and NADH. The enzyme is converted to a reduced form, and a product (NAD^+) is released. Oxygen subsequently binds to the reduced enzyme, and finally other products are released and the original oxidized holoenzyme is regenerated. On the basis of such a scheme, the initial rate equation for *m*-hydroxybenzoate hydroxylase can be expressed as

$$\frac{e}{v} = \phi_0 + \frac{\phi_{MHB}}{[MHB]} + \frac{\phi_{NH}}{[NH]} + \frac{\phi_{OX}}{[OX]} + \frac{\phi_{MHB,NH}}{[MHB][NH]} \quad (2)$$

where e is the concentration of active site, v is the observed initial rate and ϕ_0 is the reciprocal of maximal turnover rate. The terms ϕ_{MHB}, ϕ_{NH}, ϕ_{OX}, and $\phi_{MHB,NH}$ are defined as described by Dalziel (1969). Furthermore, the relationship $\phi_S = K_{m,S}\phi_0$ exists where the subscript S refers to MHB, NH, or OX and $K_{m,S}$ is the true K_m for the substrate S. These kinetic constants can be determined by secondary plots (Dalziel, 1969) as shown in the insets of Figures 3–5, and their values are summarized in Table I.

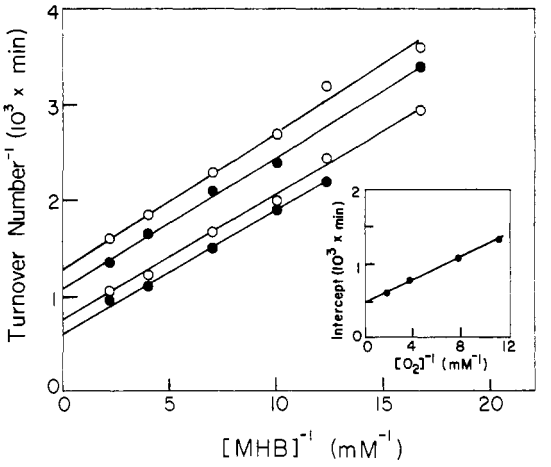

FIGURE 4: Lineweaver–Burk plots of activity vs. *m*-hydroxybenzoate concentration at a constant level of NADH and several fixed concentrations of oxygen. Reaction solutions contained 2.4 μg of enzyme, 0.6 mM NADH, and varying levels of *m*-hydroxybenzoate as indicated in 1.6 mL of 20 mM KP_i, pH 7.6. Each titration experiment was carried out at a fixed level of oxygen. The oxygen concentrations were 0.09, 0.13, 0.27, and 0.54 mM for lines from top to bottom. The inset shows a secondary plot of ordinate intercept vs. reciprocal oxygen concentration.

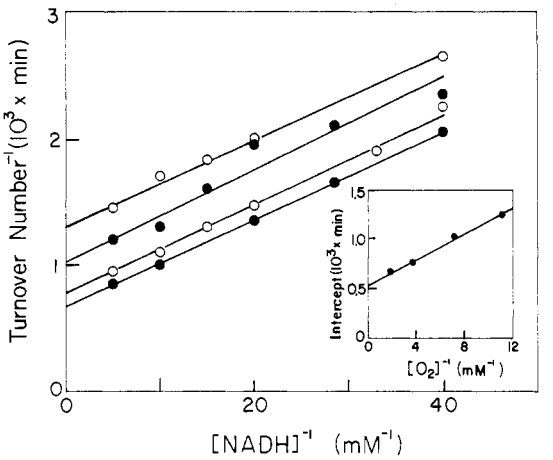

FIGURE 5: Lineweaver–Burk plots of initial velocity vs. NADH concentration at a constant amount of *m*-hydroxybenzoate and several fixed levels of oxygen. Reactions were carried out in 1.6 mL of 20 mM KP_i, pH 7.6, containing 2.4 μg of enzyme, 0.5 mM *m*-hydroxybenzoate, and varying amounts of NADH as indicated. Oxygen concentrations were 0.09, 0.14, 0.27, and 0.54 mM for lines from top to bottom. The inset shows a secondary plot of ordinate intercept vs. reciprocal oxygen concentration.

Table I: Kinetic Coefficients for *m*-Hydroxybenzoate Hydroxylase

term	value determined	term	value determined
ϕ_0 (min)	4.8×10^{-4}	$K_{m,OX}$ (M)	1.3×10^{-4}
$K_{m,MHB}$ (M)	1.9×10^{-4}	$\phi_{MHB,NH}$ (M^2 min)	7.4×10^{-12}
$K_{m,NH}$ (M)	4.6×10^{-5}		

Stereospecificity of NADH Oxidation. A reaction solution containing 20 μg of *m*-hydroxybenzoate hydroxylase, 0.49 mM *m*-hydroxybenzoate, and 0.1 mM either (4*R*)-[4-^{3}H]NADH or (4*S*)-[4-^{3}H]NADH in 20 mM KP_i, pH 7.6, was incubated

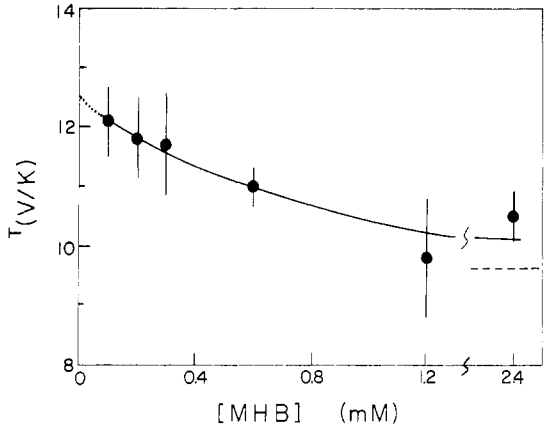

FIGURE 6: Decreases in $^{T}(V/K)$ effect of (4*R*)-[4-^{3}H]NADH at increasing levels of *m*-hydroxybenzoate. Reactions were carried out at 23 °C in 1 mL of 20 mM KP_i, pH 7.6, containing 0.1 mM (4*R*)-[4-^{3}H]NADH and varying amounts of *m*-hydroxybenzoate as indicated. Reactions were initiated by the addition of a 4-μL aliquot containing 3.2 μg of *m*-hydroxybenzoate hydroxylase. For each run, aliquots were withdrawn at four or five time points for the determination of tritiated water formation, and $^{T}(V/K)$ effects were calculated as described under Experimental Procedures. The $^{T}(V/K)$ effect at zero concentration of *m*-hydroxybenzoate was determined to be 12.5 by extrapolation. The value of $^{T}(V/K)$ at infinite concentration of *m*-hydroxybenzoate was determined to be 9.6 [shown as (--)] by the secondary plot method of Klinman et al. (1980).

at 23 °C. The reaction was monitored by following absorbance changes at 340 nm, and aliquots were taken at a desired time point for the quantitation of tritiated water formation by the same method described for tritium isotope effect measurements. At 44% oxidation of (4*R*)-[4-^{3}H]NADH, tritiated water formation was detected at a level of 1690 dpm from 50 μL of the reaction solution. On the other hand, only 110 dpm of tritiated water was detected from 50 μL of the (4*S*)-[4-^{3}H]NADH-containing sample solution at 48% completion of the reaction. These results indicate that this hydroxylase is stereospecific for the abstraction of the hydrogen at the 4*R* position of NADH. This 4*R* type of stereospecificity seems to be a common feature for flavohydroxylases (You et al., 1977; Ryerson & Walsh, 1979; Wang & Tu, 1984).

Tritium and Deuterium Isotope Effects. The $^{T}(V/K)$ effects of (4*R*)-[4-^{3}H]NADH were determined for this hydroxylase in 20 mM KP_i, pH 7.6, at different levels of *m*-hydroxybenzoate. Results obtained at 23 °C indicate that the $^{T}(V/K)$ effect gradually decreases at increasing concentrations of *m*-hydroxybenzoate (Figure 6). A value of 12.5 for $^{T}(V/K)$ at zero *m*-hydroxybenzoate concentration was obtained by extrapolation. The same data were also analyzed by a linear secondary plot following the method of Klinman et al. (1980), and the $^{T}(V/K)$ effect at infinite *m*-hydroxybenzoate concentration was calculated to be 9.6.

For the determination of deuterium isotope effects at 23 °C, enzyme activities were measured as a function of NADH or (4*R*)-[4-^{2}H]NADH concentration at saturating *m*-hydroxybenzoate. Alternatively, enzyme activities were also determined at a saturating level of NADH or (4*R*)-[4-^{2}H]NADH and various levels of *m*-hydroxybenzoate. On the basis of these results, ^{D}V, $^{D}(V/K_{NH})$, and $^{D}(V/K_{MHB})$ were calculated as described under Experimental Procedures. These values along with the value of tritium isotope effects are summarized in Table II.

Table II: Deuterium and Tritium Isotope Effects

isotope effect	value determined	isotope effect	value determined
$^{T}(V/K_{NH})_{MHB\to 0}$	12.5	$^{D}(V/K_{NH})$	3.9 ± 0.5[a]
$^{T}(V/K_{NH})_{MHB\to \infty}$	9.6	$^{D}(V/K_{MHB})$	3.0 ± 0.6[b]
^{D}V	1.4 ± 0.1[a]		
	1.6 ± 0.3[b]		

[a] Determined at 1.5 mM *m*-hydroxybenzoate and variable NADH or (4*R*)-[4-^{2}H]NADH. [b] Determined at 0.6 mM NADH or 1.3 mM (4*R*)-[4-^{2}H]NADH and variable *m*-hydroxybenzoate.

Scheme I

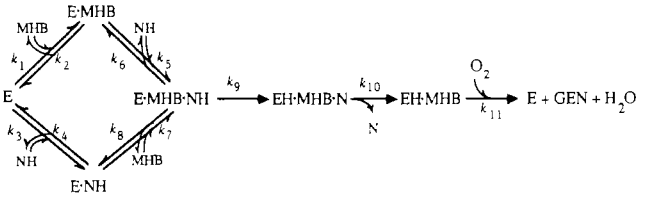

DISCUSSION

On the basis of initial rate measurements and kinetic isotope effect studies, a minimal kinetic mechanism is proposed for the *P. cepacia* *m*-hydroxybenzoate hydroxylase (Scheme I). In this scheme, E and EH are the oxidized and reduced flavohydroxylase, respectively, N is NAD^+, and GEN is the product gentisate. Other abbrevations are defined the same as before. Initial rate results shown in Figure 3 clearly indicate that NADH and *m*-hydroxybenzoate can bind to the same enzyme species to form a ternary complex. On the other hand, results shown in Figures 4 and 5 indicate that oxygen does not bind to the same enzyme form that binds *m*-hydroxybenzoate or NADH. To account for these findings, we propose that the hydroxylase first forms a ternary complex with *m*-hydroxybenzoate and NADH. The oxidized enzyme is reduced by the bound NADH, and NAD^+ is then released as the first product. Oxygen subsequently binds to and reacts with the reduced enzyme–*m*-hydroxybenzoate complex, leading to the formation of water and gentisate. After the release of these products, the oxidized holoenzyme is regenerated.

Up to this point, the question concerning the sequence of *m*-hydroxybenzoate and NADH binding has not yet been resolved. We have approached this problem by an examination of the $^{T}(V/K)$ effect of (4*R*)-[4-^{3}H]NADH as a function of *m*-hydroxybenzoate concentration. It has been previously documented that effects of the concentration of a nonlabeled substrate on the $^{T}(V/K)$ of a second tritiated substrate can be used to distinguish different kinetic mechanisms (Klinman et al., 1980; Cook & Cleland, 1981). A random sequential binding of two substrates (one labeled with tritium and the other nonlabeled) is indicated by a gradual decrease of the $^{T}(V/K)$ of the labeled substrate at increasing levels of the nonlabeled substrate, reaching a finite value above unity at infinite concentration of the nonlabeled substrate. For compulsory ordered pathways, the $^{T}(V/K)$ effect is independent of the concentration of the nonlabeled substrate if the enzyme binds the nonlabeled species first whereas the $^{T}(V/K)$ effect will be abolished at saturating concentration of the nonlabeled species if the enzyme binds the labeled substrate first. Figure 6 shows that the $^{T}(V/K)$ effect of (4*R*)-[4-^{3}H]NADH decreases at increasing concentrations of *m*-hydroxybenzoate. Furthermore, the $^{T}(V/K)$ value at infinite *m*-hydroxybenzoate concentration was determined to be 9.6 by a secondary plot method of Klinman et al. (1980). These results indicate that *m*-hydroxybenzoate and NADH bind to the hydroxylase in a random sequence.

The random binding of NADH and *m*-hydroxybenzoate is further confirmed by another approach involving the comparison of $^{D}(V/K_{NH})$ with $^{D}(V/K_{MHB})$. Kiick et al. (1986)

Table III: Formation of Flavohydroxylase Semiquinone Species

enzyme	semiquinone	method of formation	ref
bacterial luciferase	neutral	oxidation of bound $FMNH_2$ or comproportionation of $FMNH_2$ and FMN	Kurfürst et al., 1982
p-hydroxybenzoate hydroxylase	neutral	photoreduction ● (fluoro)substrates	Husain et al., 1980
liver microsomal monooxygenase	neutral	dithionite reduction or photoreduction	Beaty & Ballou, 1981
phenol hydroxylase	neutral	photoreduction ± chloride	Detmer & Massey, 1984
salicylate hydroxylase	anionic	photoreduction	Takemori et al., 1969
	neutral	photoreduction + salicylate	Takemori et al., 1969
	neutral	photoreduction + salicylate	White-Stevens et al., 1972
	anionic	electrochemical reduction	M. Stankovich and S.-C. Tu, unpublished results
3-hydroxybenzoate 6-hydroxylase	neutral	photoreduction ± *m*-hydroxybenzoate	this work

have pointed out that a random binding mechanism can be concluded for any bi- or tersubstrate reaction if one observes finite $^{D}(V/K)$ values for all substrates. In the present case with *m*-hydroxybenzoate hydroxylase, values of 3.0 and 3.9 were obtained for $^{D}(V/K_{MHB})$ and $^{D}(V/K_{NH})$, respectively (Table II). Therefore, these results present another line of evidence in support of the mechanism for random binding of NADH and *m*-hydroxybenzoate. In all, the scheme proposed as the minimal kinetic mechanism for *m*-hydroxybenzoate hydroxylase is well justified.

Additional important information can be revealed by an analysis of deuterium isotope effects. In this study, the intrinsic isotope effect $^{D}k_9$ has not been directly determined. As an approximation, $^{D}k_9$ is estimated to be 10.2 according to the relationship (Northrop, 1975)

$$\frac{^{D}(V/K) - 1}{^{T}(V/K) - 1} = \frac{^{D}k_9 - 1}{(^{D}k_9)^{1.44} - 1} \qquad (3)$$

The substantial reduction of $^{D}k_9$ to a value of 1.4–1.6 for ^{D}V indicates that at least one slow reaction step must exist after the isotope-sensitive step of k_9. Furthermore, a comparison of $^{D}k_9$, $^{D}(V/K_{NH})$, and $^{D}(V/K_{MHB})$ can enable us to evaluate the randomness of the mechanism (Ahn & Klinman, 1983). Kinetic expressions can be derived on the basis of Scheme I for the following deuterium isotope effects:

$$^{D}(V/K_{NH}) = (^{D}k_9 + k_9/k_6)/(1 + k_9/k_6) \qquad (4)$$

$$^{D}(V/K_{MHB}) = (^{D}k_9 + k_9/k_8)/(1 + k_9/k_8) \qquad (5)$$

Using 10.2 for $^{D}k_9$ and experimentally determined values for $^{D}(V/K_{MHB})$ and $^{D}(V/K_{NH})$, a ratio of $k_6/k_8 = 1.7$ is obtained following eq 4 and 5. This indicates that NADH dissociates from the E·MHB·NH ternary complex with a rate slightly faster than that for the dissociation of *m*-hydroxybenzoate. The randomness for the binding of NADH and *m*-hydroxybenzoate is thus quantitatively expressed.

We have previously demonstrated that the relationship shown in eq 3 indeed holds for salicylate hydroxylase (Wang & Tu, 1984). Therefore, the estimation of $^{D}k_9$ for *m*-hydroxybenzoate hydroxylase according to this relationship is not without any precedent. However, it should also be noted that if the isotope-sensitive step is reversible and prior to the first irreversible step in the reaction pathway, as in the case of *p*-hydroxybenzoate hydroxylase (Ryerson et al., 1982), the observed value of $^{T}(V/K)$ would be significantly larger than that calculated following eq 3 and with experimentally determined values of $^{D}(V/K)$ and ^{D}k. This also means that the true value of ^{D}k would be smaller than that predicted on the basis of eq 3 and experimentally determined $^{D}(V/K)$ and $^{T}(V/K)$. If *m*-hydroxybenzoate hydroxylase behaves similarly, the true value of $^{D}k_9$ should thus be smaller than 10.2. However, this has little effect on the randomness of the mechanism. For the purpose of discussion, let us assume a value of 6 for $^{D}k_9$. The corresponding ratio of k_6/k_8 would than be 2.1. Still, there is only a small preference for NADH over *m*-hydroxybenzoate for dissociation from the ternary complex.

A 4a-hydroxyperoxyflavin species appears to be a key intermediate for all flavohydroxylases. In chemical model studies, strong evidence has been presented for a mechanism of 4a-hydroperoxyflavin formation that involves a rate-limiting one-electron transfer from dihydroflavin to oxygen and a subsequent reaction between flavin semiquinone and superoxide anion (Bruice, 1984). However, whether flavin semiquinone is involved in the catalysis of flavohydroxylases is still unclear. In this case, a stable neutral flavin semiquinone species was formed by photoreduction of *P. cepacia m*-hydroxybenzoate hydroxylase in the absence or presence of *m*-hydroxybenzoate (Figure 2) whereas no flavin radical was detected upon reduction by NADH in the presence of *m*-hydroxybenzoate (Figure 1). Conditions for the NADH reduction corresponded to those for the reductive half of the catalytic reaction of this hydroxylase. In such a case, the formation of flavin semiquinone is apparently thermodynamically unfavorable. As summarized in Table III, the formation of flavin radicals, both neutral and anionic, has also been detected for several other flavohydroxylases. However, direct evidence for an intermediacy of flavin semiquinone in hydroxylase catalysis has not yet been established for any of these cases.

Acknowledgments

We are grateful to Dr. J. P. Klinman for kindly providing the BASIC version of the steady-state kinetic analysis computer programs and to Dr. C Thorpe for the generous gift of an anaerobic titration apparatus.

Registry No. NH, 58-68-4; MHB, 99-06-9; OX, 7782-44-7; 3-hydroxybenzoate 6-hydroxylase, 51570-26-4.

References

Ahn, N., & Klinman, J. P. (1983) *Biochemistry 22*, 3096–3106.

Ball, S., & Bruice, T. C. (1980) *J. Am. Chem. Soc. 102*, 6498–6503.

Ballou, D. P. (1984) in *Flavins and Flavoproteins* (Bray, R. C., Engel, P. C., & Mayhew, S. G., Eds.) pp 605–618, de Gruyter, Berlin.

Beaty, N. B., & Ballou, D. P. (1981) *J. Biol. Chem. 256*, 4611–4618.

Bruice, T. C. (1984) in *Flavins and Flavoproteins* (Bray, R. C., Engel, P. C., & Mayhew, S. G., Eds.) pp 45–55, de Gruyter, Berlin.

Cleland, W. W. (1979) *Methods Enzymol. 63*, 103–138.

Cook, P. F., & Cleland, W. W. (1981) *Biochemistry 20*, 1790–1796.

Dalziel, K. (1969) *Biochem. J. 114*, 547–556.

Detmer, K., & Massey, V. (1984) *J. Biol. Chem. 259*, 11265–11272.
Groseclose, E. E., & Ribbons, D. W. (1973) *Biochem. Biophys. Res. Commun. 55*, 897–903.
Hastings, J. W. (1978) *Methods Enzymol. 576*, 125–135.
Husain, M., Entsch, B., Ballou, D. P., Massey, V., & Chapman, P. J. (1980) *J. Biol. Chem. 255*, 4189–4197.
Kemal, C., & Bruice, T. C. (1976) *Proc. Natl. Acad. Sci. U.S.A. 73*, 995–999.
Kemal, C., Chan, T. W., & Bruice, T. C. (1977) *Proc. Natl. Acad. Sci. U.S.A. 74*, 405–409.
Kiick, D. M., Harris, B. G., & Cook, P. F. (1986) *Biochemistry 25*, 227–236.
Klinman, J. P., Humphries, H., & Voet, J. G. (1980) *J. Biol. Chem. 255*, 11648–11651.
Kurfürst, M., Ghisla, S., Presswood, R., & Hastings, J. W. (1982) *Eur. J. Biochem. 123*, 355–361.
Lowry, O. H., Rosebrough, N. J., Farr, A. L., & Randall, R. J. (1951) *J. Biol. Chem. 193*, 265–275.
Massey, V., & Swoboda, B. E. P. (1963) *Biochem. Z. 338*, 474–484.
Massey, V., & Palmer, G. (1966) *Biochemistry 5*, 3181–3189.
Massey, V., & Hemmerich, P. (1975) *Enzymes (3rd Ed.) 12*, 191–252.
Northrop, D. B. (1975) *Biochemistry 14*, 2644–2651.
Oppenheimer, N. J., Arnold, L. J., & Kaplan, N. O. (1971) *Proc. Natl. Acad. Sci. U.S.A. 68*, 3200–3205.
Ryerson, C. C., & Walsh, C. (1979) *J. Biol. Chem. 254*, 4349–4351.
Ryerson, C. C., Ballou, D. P., & Walsh, C. (1982) *Biochemistry 21*, 1144–1151.
Takemori, S., Yasuda, H., Mihara, K., Suzuki, K., & Katagiri, M. (1969) *Biochim. Biophys. Acta 191*, 69–76.
Wang, L.-H., & Tu, S.-C. (1984) *J. Biol. Chem. 259*, 10682–10688.
Wang, L.-H., Hamzah, R. Y., Yu, Y., & Tu, S.-C. (1987) *Biochemistry* (preceding paper in this issue).
White-Stevens, R. H., Kamin, H., & Gibson, Q. H. (1972) *J. Biol. Chem. 247*, 2371–2381.
Williams, C. H., Jr., Arscott, L. D., Matthews, R. G., Thorpe, C., & Wilkinson, K. D. (1979) *Methods Enzymol. 62*, 185–198.
You, K.-S., Arnold, L. J., Jr., & Kaplan, N. O. (1977) *Arch. Biochem. Biophys. 180*, 550–554.

Ca^{2+}- and Calmodulin-Dependent Stimulation of Smooth Muscle Actomyosin Mg^{2+}-ATPase by Fodrin†

Chiayeng Wang,‡ Philip K. Ngai,§ Michael P. Walsh,‖ and Jerry H. Wang*,⊥

Department of Medical Biochemistry and Cell Regulation Group, The University of Calgary, Calgary, Alberta, Canada T2N 4N1

Received July 9, 1986; Revised Manuscript Received October 27, 1986

ABSTRACT: Fodrin, a spectrin-like actin and calmodulin binding protein, was purified to electrophoretic homogeneity from a membrane fraction of bovine brain. The effect of fodrin on smooth muscle actomyosin Mg^{2+}-ATPase activity was examined by using a system reconsituted from skeletal muscle actin and smooth muscle myosin and regulatory proteins. The simulation of actomyosin Mg^{2+}-ATPase by fodrin showed a biphasic dependence on fodrin concentration and on the time of actin and myosin preincubation at 30 °C. Maximal stimulation (50–70%) was obtained at 3 nM fodrin following 10 min of preincubation of actin and myosin. This stimulation was also dependent on the presence of tropomyosin. In the absence of myosin light chain kinase, the fodrin stimulation of Mg^{2+}-ATPase could not be demonstrated with normal actomyosin but could be demonstrated with acto–thiophosphorylated myosin, suggesting that fodrin stimulation depends on the phosphorylation of myosin. Fodrin stimulation was shown to require the presence of both Ca^{2+} and calmodulin when acto–thiophosphorylated myosin was used. These observations suggest a possible functional role of fodrin in the regulation of smooth muscle contraction and demonstrate an effect on Ca^{2+} and calmodulin on fodrin function.

Fodrin is a protein whose physical, biochemical, and immunological properties are similar to those of spectrin, one of the major cytoskeletal components found in erythrocytes (Goodman et al., 1981). It is composed of two nonidentical subunits (M_r 240000 and 235000) intertwined in a filamentous form in the cell. Purified fodrin appears to exist as a tetramer consisting of two heterodimers joined head to head under physiological conditions (Bennett et al., 1982). It binds actin filaments and undergoes Ca^{2+}-dependent association with calmodulin (Palfrey et al., 1982). Some investigators (Kakiuchi et al., 1982; Davies & Klee, 1981) purified fodrin from mammalian brain as a calmodulin binding protein without knowing its relationship to spectrin; therefore, it was also called calmodulin binding protein I or calspectin.

Fodrin is concentrated in regions underlying the plasma membrane of neuronal and a wide variety of nonneuronal cells and tissues [for a review, see Goodman & Zagon (1984)]. It

† This work was supported by grants from the Alberta Heritage Foundation for Medical Research and the Medical Research Council of Canada.
‡ Medical Research Council Studentship Awardee.
§ Alberta Heritage Foundation for Medical Research Studentship Awardee.
‖ Alberta Heritage Foundation for Medical Research Scholar.
⊥ Alberta Heritage Foundation for Medical Research Medical Scientist.

0006-2960/87/0426-1110$01.50/0